



# EXPERIMENTAL

The experiments were carried out on  $\text{Cd}_{0.7}\text{Hg}_{0.3}\text{Te}/\text{HgTe}/\text{Cd}_{0.7}\text{Hg}_{0.3}\text{Te}$  single QWs of 21 nm width. The structures were grown on GaAs substrates with surface orientation (013), by means of a modified Molecular Beam Epitaxy method [18]. Samples with electron densities of  $9 \cdot 10^{11} \text{ cm}^{-2}$  and mobility  $2.5 \cdot 10^4 \text{ cm}^2/\text{Vs}$  are studied at room temperature. We used square shaped samples of  $5 \cdot 5 \text{ mm}^2$  size. Two pairs of contacts (along directions x and y) was centered in the middle of cleaved edges parallel to the intersection of the (013) plane and cleaved edge face  $\bar{1}10g$  (see the inset to Fig. 1). To demonstrate the detector operation in the mid-infrared spectral range we used a Q-switched  $\text{CO}_2$  laser covering the spectrum from 9.2 to 10.8  $\mu\text{m}$  with peak power  $P$  of about 1 kW and pulsed TEA- $\text{CO}_2$  laser generating single 100 ns pulses of power up to 100 kW [3]. Besides gas lasers we used the output from the free electron laser "FELIX" at FOM-Rijnhuizen in the Netherlands at wavelengths between 5  $\mu\text{m}$  and 17  $\mu\text{m}$  and power about 100 kW [19]. Making use of the frequency tunability and short pulse duration of this laser we obtain the spectral behaviour of the detector responsivity and demonstrated its time resolution. The output pulses of light from FELIX were chosen to be 3 ps long, separated by 40 ns, in a train (or "macro-pulse") of duration of 7  $\mu\text{s}$ . The macro-pulses had a repetition rate of 5 Hz. For optical excitation in the terahertz range we used a cw optically pumped  $\text{CH}_3\text{OH}$  laser with radiation wavelength of 118  $\mu\text{m}$  and power  $P$  of about 10 mW and high power pulsed optically pumped  $\text{NH}_3$ ,  $\text{D}_2\text{O}$ , and  $\text{CH}_3\text{F}$  lasers [3]. Several lines of the pulsed laser with power ranging from 100 W to 100 kW in the wavelength range between 76  $\mu\text{m}$  and 496  $\mu\text{m}$  have been applied.

To vary the ellipticity of the laser beam we used  $\lambda/4$  plates made of x-cut crystalline quartz in the terahertz range and a Fresnel rhomb in the mid-infrared. The light polarization was varied from linear to elliptical. Rotating the polarizer varies the helicity of the light,  $P_{\text{circ}} = \sin 2\theta$ , from  $P_{\text{circ}} = -1$  (left-handed circular,  $-$ ) to  $P_{\text{circ}} = +1$  (right-handed circular,  $+$ ) where  $\theta$  is the angle between the initial linear polarization and the optical axis (c-axis) of the polarizer. In Fig. 1 (top) the shape of the polarization ellipse and the handedness of the radiation are shown for various angles  $\theta$ .

Photogalvanic effects applied here for radiation detection generate an electric current which we measure in homogeneously irradiated unbiased samples. The current is converted into a signal voltage by load resistors. The signal voltages were picked up from the detector across a  $R_L = 50 \Omega$  load resistor for short radiation pulses. For cw irradiation we use a load resistance of 1 M $\Omega$ , which is much higher than the sample resistance. For pulsed lasers

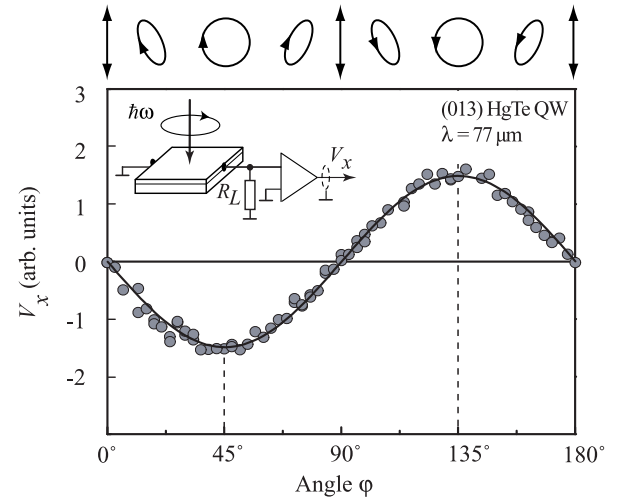


FIG. 1: Helicity dependence of the photoresponse normalized by the radiation power  $V_x = P$  in a (013)-grown HgTe QW at room temperature. The signals are obtained at  $\lambda = 77 \mu\text{m}$  applying pulsed radiation of  $\text{NH}_3$  THz laser. The full line is a fit after Eq. (1). The inset shows the experimental geometry. On top of the figure polarization ellipses corresponding to various phase angles  $\theta$  are plotted viewing from the direction toward which the wave approaches.

the signals were fed into amplifiers with voltage amplification by a factor of 100 and a bandwidth of 300 MHz and were recorded by a digital broadband (1 GHz) oscilloscope. For time resolved measurements the signal was picked up directly from the sample without amplification. For detection of cw laser radiation we modulated our beam with a chopper at modulation frequency 225 Hz and used a low-noise pre-amplifier (100 times voltage amplification) and a lock-in-amplifier for signal recording. We note that in this low modulation frequency case the high time resolution of the set-up is not required.

## DETECTION OF THE HELICITY APPLYING HgTe QWs

With illumination of HgTe samples at normal incidence we detected in the in-plane x-direction a helicity dependent current signal. This is shown in Fig. 1 for a measurement at room temperature obtained at 77  $\mu\text{m}$  wavelength of a pulsed  $\text{NH}_3$  laser. Note that the measurement is d.c. coupled and no background subtraction has occurred. The signal changes direction if the circular polarization is switched from left to right-handed ( $-$  to  $+$  as shown in Fig. 1) and vice versa. The helicity dependence and in particular the change of sign demonstrate that the observed current  $j_x$  is due to the CPGE [3]. The voltage signal resulting from the photocurrent  $V_x / j_x$  is well described by

$$V_x^{\text{HgTe}} = S(\theta) P E_{\text{circ}}; \quad (1)$$

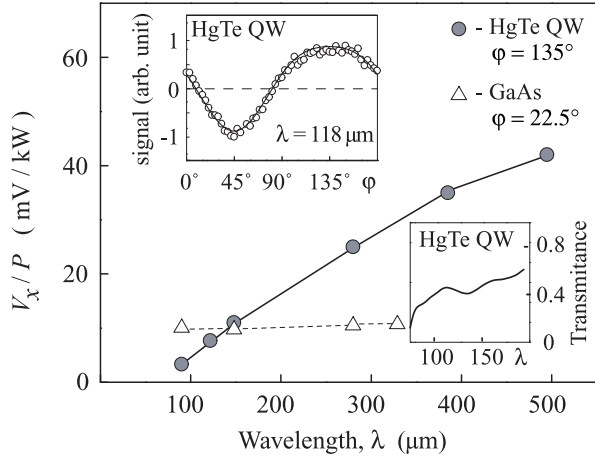


FIG. 2: CPGE spectrum of HgTe QW (full circles) in the THz-range normalized by power incident on the sample for circularly polarized radiation ( $\phi' = 135^\circ$ ). Top inset shows the helicity dependence obtained in HgTe QW applying radiation of a cw  $\text{CH}_3\text{OH}$  laser at  $\lambda = 118 \mu\text{m}$ . Full line in the inset is the  $t$  after Eq. (3). Bottom inset shows transmittance spectrum obtained by FTIR spectroscopy. Triangles show the spectrum of bulk GaAs sample in response to the elliptically polarized radiation. The data are given for angles  $\phi' = 22.5^\circ$  corresponding to the maximum of the voltage signal.

where  $S(\phi')$  denotes the strength of CPGE at radiation frequency  $\omega$ , and, consequently, the sensitivity of this detector unit. The photogalvanic current is described by the phenomenological theory. It can be written as a function of the electric component of the radiation field  $E$  and the propagation direction  $\hat{e}$  in the following form [4, 17]

$$j = \sum_i \hat{e}_i P_{\text{circ}} \mathcal{E}_i^j + \sum_i (\mathbf{E} \cdot \mathbf{E} + \mathbf{E} \cdot \mathbf{E}^*) j_i; \quad (2)$$

where the first term on the right hand side being proportional to the helicity or circular polarization degree  $P_{\text{circ}}$  of the radiation represents the CPGE while the second term corresponds to the linear photogalvanic effect (LPGE) [3] which may be superimposed to the CPGE. The indices  $i, j, k$  run over the coordinate axes  $x, y, z$ . The second rank pseudotensor  $\mathcal{E}_i^j$  and the third rank tensor  $j_i$  symmetric in the last two indices are material parameters. The (013)-oriented QWs belong to the trivial point group  $C_1$  lacking any symmetry operation except the identity. Hence symmetry does not impose any restriction on the relation between irradiation and photocurrent. All components of the tensor  $\mathcal{E}_i^j$  and the pseudotensor  $j_i$  may be different from zero. Equation (2) yields for normal incidence of the radiation the angle  $\phi'$  dependence of the photosignal  $V_x / j_k$

$$V_x/P = S(\phi') \sin 2\phi' + b(\phi') \sin 4\phi' + c(\phi') \cos 4\phi' + d(\phi'); \quad (3)$$

where  $S(\phi'), b(\phi'), c(\phi'),$  and  $d(\phi')$  can be consistently expressed by components of the tensors  $\mathcal{E}_i^j$  and  $j_i$ .

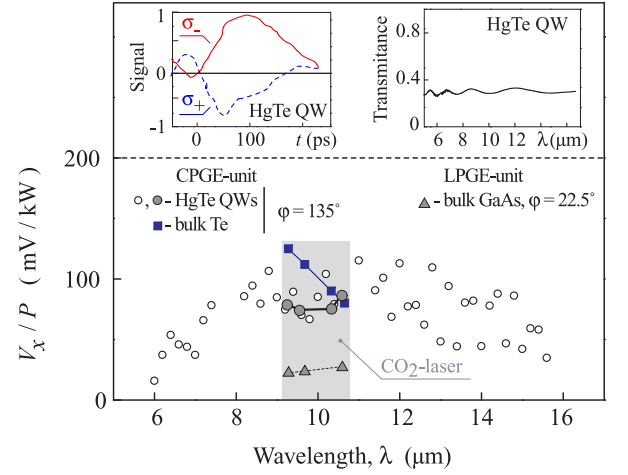


FIG. 3: CPGE spectrum of HgTe QW and Te bulk crystal obtained in response to the terahertz-infrared circular polarized radiation and normalized by power incident on the sample for circularly polarized radiation. The data are obtained for angles  $\phi' = 135^\circ$  applying Q-switched  $\text{CO}_2$  laser (full circles) and free electron laser FELIX ( $\lambda = 9 \mu\text{m}$ ) (open circles). The data of Te are plotted by squares. Triangles represent spectral response of the LPGE bulk GaAs unit obtained by pulsed TEA- $\text{CO}_2$  laser radiation. The data are given for angles  $\phi' = 22.5^\circ$  corresponding to the maximum of the voltage signal. The shadow area indicates the spectral range of a  $\text{CO}_2$  laser. Left and right insets show the CPGE temporal response of HgTe QWs to sub-ps infrared pulses of FELIX ( $\lambda = 9 \mu\text{m}$ ) and the transmittance spectra obtained by FTIR spectroscopy, respectively.

ned in Eq. (2) [20]. While at most wavelengths we found that the first term in Eq. (3) dominates (see Fig. 1), at some wavelengths we also find a small polarization independent current offset and a slight distortion of the sine-shape of the  $V_x$  versus  $\phi'$  curve. This deviation from the  $\sin 2\phi'$  behaviour is demonstrated in the inset of Fig. 2 for  $118 \mu\text{m}$  wavelength of the cw  $\text{CH}_3\text{OH}$  laser. The solid line in this inset is calculated after Eq. (3) yielding a good agreement to the experiment. Note, however, that for a technical application as an ellipticity detector described here it is desirable to have samples with dominating CPGE term being simply proportional to  $P_{\text{circ}}$  like the photoresponse in Fig. 1. For all wavelengths this goal could be achieved by using technologically available (112)-grown samples [6]. The reason is the higher symmetry of such structures. In (013)-oriented samples investigated in our work the CPGE current can have arbitrary direction and, in fact, the projection of the current on the connecting line between the contacts is measured. Furthermore three LPGE current contributions are allowed due to the low symmetry of the samples. In contrast, in (112)-grown structures the current direction for normal incidence is bound to the  $[110]$ -crystallographic direction. This is because such samples belong to the  $C_s$  point group forcing the CPGE current to a direction

normal to the mirror reflection plane. This feature makes the preparation of samples with dominating CPGE for all wavelengths possible. Picking up the signal from  $[110]$ -direction should increase the sensitivity and smoothen the spectral dependence.

In Fig. 2 and Fig. 3 the spectral dependence of the CPGE is shown for the infrared and THz ranges, respectively. The measurements are carried out at room temperature at normal incidence of radiation and for circularly polarized radiation ( $\varphi = 135^\circ$ ) where the CPGE signal is maximal. In the THz range molecular lasers were applied while the measurements in the infrared range were performed using FELIX (open circles in Fig. 3) and a Q-switched  $\text{CO}_2$  laser (full circles in Fig. 3). In the infrared range CPGE in HgTe QWs does not show much dispersion for between 8 and 14  $\mu\text{m}$  while in the THz range the photocurrent rises significantly with increasing wavelength. The spectral behaviour of the signal is mainly caused by the mechanism involved in the radiation absorption, interband in the mid-infrared range and Drude-like in the terahertz range. The sensitivity in the mid-infrared range being of the order of  $80 \text{ mV/kW}$  is comparable with that of photon drag detectors widely applied for detection of infrared laser radiation [3, 21, 22]. Comparing sensitivities of HgTe QW and GaAs QW devices in the THz range we obtain that a detector element made of one single HgTe quantum well ( $S = 10 \text{ mV/kW}$  for  $\lambda = 148 \mu\text{m}$ ) has about 100 times higher sensitivity per quantum well than devices based on GaAs QWs [23]. The sensitivity of HgTe QW based devices can be further improved simply by using a larger number of QWs.

To determine the time resolution of our device we used 3 ps pulses of FELIX. The left inset in Fig. 3 shows that the response time is at most 100 ps. We attribute the observed time constant to the bandwidth of our electronic set-up. A fast response is typical for photogalvanics where the signal decay time is determined by the momentum relaxation time [3, 17] being in our samples of the order of 0.3 ps at room temperature. As a large dynamic range is important for detection of laser radiation, we investigated the dependence of the sensitivity of the detection system on the radiation intensity applying cw and high-power pulsed radiation. We observed that the ellipticity detector at homogeneous irradiation of the whole sample remains linear up to  $2 \text{ MW/cm}^2$  over more than nine orders of magnitude.

In a further experiment we checked the variation of the sensitivity due to a deviation from normal incidence of radiation. Measurements at oblique incidence demonstrate that the CPGE current attains maximum at normal incidence. This is shown in Fig. 4 for angles of incidence  $\theta_0$  in the range  $\pm 30$  degrees at a wavelength  $\lambda = 148 \mu\text{m}$  and for circularly polarized light. We find that the sensitivity is reduced at a deviation from normal incidence. This behaviour follows from Eq. (2) yielding  $j / t_p \propto \cos \theta_0$  where  $t_p$  and  $t_s$  are the Fresnel transmission coefficients

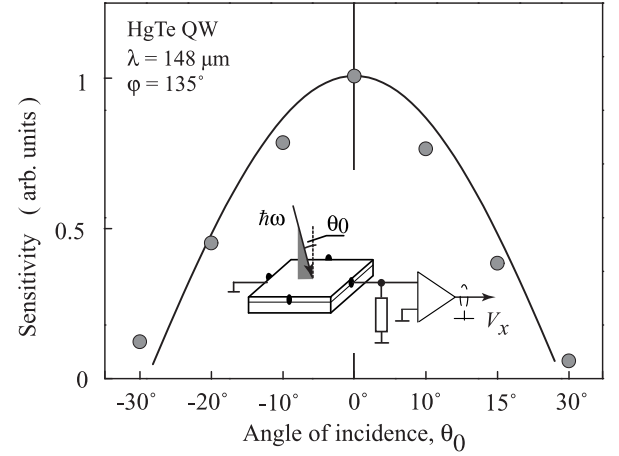


FIG. 4: Sensitivity of the (013)-oriented HgTe QW CPGE-detector unit as a function of the angle of incidence for circularly polarized radiation. The data are shown for the rotation of the angle of incidence in  $(xz)$ -plane. Full line shows the fit of the data to the phenomenological theory taken into account besides CPGE an additional contribution of the circular photon drag effect [25].

for s- and p-polarized light, and  $\theta_1$  is the refraction angle given by  $\sin \theta_1 = \sin \theta_0 n_1$ , where  $n_1$  is the refraction index [24]. Experimentally, however, we observed that in our samples the photocurrent drops more strongly with increasing  $\theta_0$  than expected from Fresnel's formula. We attribute this effect to a superposition of CPGE with the circular photon drag effect [25] at oblique incidence. Because both effects are proportional to  $P_{\text{circ}}$  and have the same temporal kinetic, this superposition does not compromise the detector's functionality.

#### DETECTION OF THE ELLIPSE'S AZIMUTH ANGLE WITH BULK GaAs

To obtain all Stokes parameters besides the CPGE which provides an information on the radiation helicity, an additional detector element for determination of the ellipse azimuth is needed [1]. In our previous work aimed at the detection of THz radiation we used for this purpose the linear photogalvanic effect in SiGe QWs. The LPGE in SiGe structures is also detected in the mid-infrared range [26]. However, the signal is rather small and the response is obtained only at wavelength about  $10 \mu\text{m}$  under resonant intersubband transitions. To search for other materials, with the aim to increase the sensitivity and to extend the spectral range of the detector, we analyze here the LPGE in bulk GaAs crystals. Bulk GaAs crystals belong to  $T_d$  point group symmetry. While the CPGE in materials of this symmetry is forbidden, an LPGE current can be generated applying linearly or elliptically polarized radiation.

We prepared (111)-oriented p-type GaAs samples of



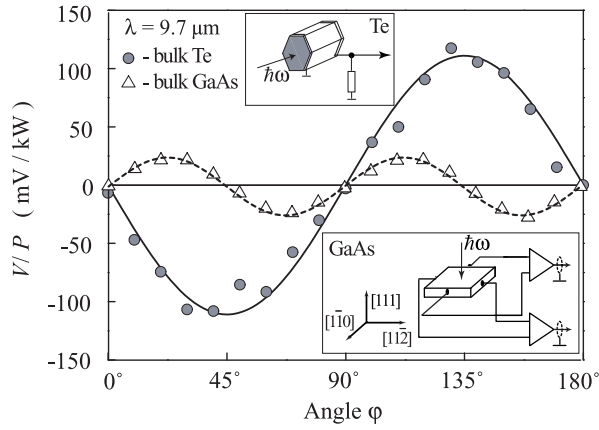


FIG. 5: Helicity dependence of the photoresponse normalized by the radiation power  $V/P$  in bulk Te (circles) and bulk GaAs (triangles) samples at room temperature. The signals are obtained at  $\lambda = 9.7 \mu\text{m}$  applying pulsed TEA  $\text{CO}_2$  laser radiation. Full and dashed lines are fits after  $V_z = P / \sin 2'$  and  $V_{[110]} = P / \sin 4'$  for Te and GaAs, respectively. Insets show the experimental geometry for both samples. In the GaAs-detector unit the signal of each contact pair is fed into a differential amplifier operating against ground.

5.5  $2 \text{ mm}^3$  sizes with a contact pair along  $x$   $k$   $[110]$  and  $y$   $k$   $[112]$  axes as sketched in Fig. 5. We used materials with free hole densities of about  $2.3 \cdot 10^{16} \text{ cm}^{-3}$  like it previously been used for detection of the plane of polarization of linearly polarized radiation [27]. In our measurements we aligned the  $[110]$ -side of the sample parallel to the light polarization vector of the laser beam. The current of each contact pair is fed into a differential amplifier operating against ground.

According to Eq. (2) irradiation with polarized radiation propagating in the  $[111]$  crystallographic direction yield transverse signals given by

$$\begin{aligned} \frac{V_{[112]}}{P} &= C(!) \frac{(E_x^2 - E_y^2)}{E^2}; \\ \frac{V_{[110]}}{P} &= C(!) \frac{(E_x E_y + E_y E_x)}{E^2}; \end{aligned} \quad (4)$$

where  $C(!)$  is a constant factor being proportional to the only one non-zero component of the third rank tensor [24].

In our experimental set-up where the radiation ellipticity is varied by the rotation of the quarter-wave plate by an angle  $'$ ,  $(E_x^2 - E_y^2)/E^2 = (1 + \cos 4')/2$  and  $(E_x E_y + E_y E_x)/E^2 = \sin 4' = 2$ . Applying infrared radiation we clearly detected both dependences of the photosignal. Figure 5 shows the angle  $'$  dependence of  $V_{[110]} = P$  obtained applying radiation at  $\lambda = 9.7 \mu\text{m}$ .

From the angle  $'$  dependence we obtain the LPGE constant  $C(!)$  which determines the detector element sensitivity providing the calibration of the device. Figure 3 shows the spectral behaviour of the constant  $C(!)$  at infrared wavelengths obtained by the Q-switched  $\text{CO}_2$

laser. The sensitivity of the order of  $20 \text{ mV/kW}$  is measured for the angle  $' = 22.5^\circ$  at which signal achieves its maximum value. This value is comparable to that of the HgTe QW CPGE-detector unit. We also obtained a considerable signal in the terahertz range characterized by the same angle  $'$  dependences. Here the sensitivity at  $148 \mu\text{m}$  is also comparable to that of the HgTe QW CPGE-detector unit and is about 20 times higher than that measured previously in SiGe QWs [2].

To obtain the Stokes parameters of a radiation field the signals from HgTe QW and bulk GaAs must be measured simultaneously. In the work on a THz ellipticity detector we simply stacked the CPGE- and the LPGE-detector units. This arrangement is only possible if the first of the two elements is practically transparent to the incident radiation. Therefore we carried out FTIR measurements of the transmission of HgTe QW. These data are shown in insets to Figs. 3 and 2. The essential result is that the sample is almost transparent and can be used in a stacked configuration. The transmittance in the whole spectral range is about 30-40 percents which just corresponds to the reflectivity of the sample. The oscillations in the spectrum are due to interference in the plane-parallel transparent semiconductor slab. The magnitude of the reflection can be reduced by anti-reflection coatings improving the sensitivity of the detector system.

## STOKES PARAMETERS

From the signals obtained by the CPGE-detector unit (HgTe QW) and by the LPGE-unit (bulk GaAs) it follows that simultaneous measurements of two signals allow one the determination of the Stokes parameters which completely characterize the state of polarization of the radiation field. The Stokes parameters defined according to [28] are directly measured in our detector units yielding

$$\begin{aligned} s_0 &= E^2; \\ \frac{s_1}{s_0} &= \frac{E_x^2 - E_y^2}{E^2} = \frac{V_{[112]}^{\text{GaAs}}}{P \cdot C(!)}; \\ \frac{s_2}{s_0} &= \frac{E_x E_y + E_y E_x}{E^2} = \frac{V_{[110]}^{\text{GaAs}}}{P \cdot C(!)}; \\ \frac{s_3}{s_0} &= \frac{i(E_y E_x - E_x E_y)}{E^2} = P_{\text{circ}} = \frac{V_x^{\text{HgTe}}}{P \cdot S(!)}; \end{aligned} \quad (5)$$

where the parameter  $s_0 / P$  does not contain information about the polarization state and determines the radiation intensity.

## CPGE UNIT BASED ON BULK Te

Finally we investigated CPGE in another narrow band semiconductor | bulk Te | with respect to its appli-

cability in an ellipticity detector and compare the results with the data on HgTe QW structures. In fact bulk Te was the first material in which the CPGE was detected [29]. Single crystal Te belongs to the point group  $D_3$  where second rank pseudotensors are diagonal in a coordinate system with  $z$  along the trigonal crystallographic axis. This axis is also the growth direction of bulk crystals. The macroscopic shape of Te is hexagonal. Thus, irradiating a sample along  $z$  direction generates a longitudinal current along this axis. Equation (2) yields for the photovoltage  $V_z / j_z$  in Te [30]

$$V_z = P = S'(\omega) P_{\text{circ}} \quad (6)$$

In order to measure this current we prepared two contacts around circumferences of hexagonal prism shaped specimens, see inset in Fig. 5. We used p-doped tellurium crystals which at room temperature have the hole concentration of about  $3.5 \cdot 10^{16} \text{ cm}^{-3}$ . The samples were of 11.5 mm long and had a cross section of  $20 \text{ mm}^2$ . Illuminating the crystal along  $z$  axis by mid-infrared radiation we detected a polarization dependent signal reversing polarity upon switching the radiation helicity (see Fig. 5). In our experimental set-up the radiation helicity is varied by the rotation of the quarter-wave plate by an angle  $\theta'$  according to  $P_{\text{circ}} = \sin 2\theta'$ . The signal  $V_z$  is well described by this dependence. The possible contribution of the longitudinal photon drag effect is vanishingly small in our samples at room temperature in agreement to Ref. 29. Figure 3 shows the spectral behaviour of the sensitivity of the Te sample obtained for circularly polarized radiation. Our investigations demonstrate that in this material the sensitivity in the mid-infrared is about three times higher than that observed for a HgTe single QW (Fig. 3). The data prove that bulk Te can be used as CPGE detector unit in the mid-infrared. However, application of multiple HgTe QWs for which the sensitivity scales linearly with the number of QWs should provide a sensitivity substantially higher than that of Te making HgTe QWs preferable for ellipticity detection. In the THz-range we did not find a CPGE signal in Te even when applying the highest available radiation power.

## CONCLUSION

We demonstrated that the application of novel narrow gap semiconductor low dimensional materials allows all-electric detection of the Stokes parameters of elliptically polarized radiation from the mid-infrared to the THz range. The sensitivity and linearity of the detection system developed here has been found to be sufficient to characterize the polarization of laser radiation from low-power cw-lasers to high-power laser pulses. The short relaxation time of free carriers in semiconductors at room temperature makes it possible to detect sub-ns laser pulses demonstrated with the free-electron-laser FELIX.

Finally we note that a further increase of the sensitivity may be obtained by using multiple QWs and technologically available (112)-grown samples.

We thank S.A. Tarasenko, E.L. Ivchenko and V.V. Bel'kov for useful discussions. The financial support of the DFG and RFBR is gratefully acknowledged. Work of L.E.G. is also supported by "Dynasty" Foundation | IC FPM and President grant for young scientists.

- 
- [1] S.D. Ganichev, J. Klemm, W. Weber, S.N. Danilov, D. Schuh, Ch. Gerl, W. Wegscheider, D. Bougeard, G. Abstreiter, and W. Prettl, *Appl. Phys. Lett.* 91, 091101 (2007).
  - [2] S.D. Ganichev, W. Weber, J. Klemm, S.N. Danilov, D. Schuh, W. Wegscheider, Ch. Gerl, D. Bougeard, G. Abstreiter and W. Prettl *J. Appl. Physics* 103, 114504 (2008).
  - [3] S.D. Ganichev and W. Prettl, *Intense Terahertz Excitation of Semiconductors* (Oxford University Press, Oxford, 2006).
  - [4] E.L. Ivchenko, *Optical Spectroscopy of Semiconductor Nanostructures* (Alpha Science International, Harrow, UK, 2005).
  - [5] A. Pfeufer-Jeschke, F. Goschenhofer, S.J. Cheng, V. Latussek, J. Gerschütz, C.R. Becker, R.R. Gerhardt, G. Landwehr, *Physica B* 256-258, 486 (1998).
  - [6] X.C. Zhang, A. Pfeufer-Jeschke, K. Ortner, V. Hock, H. Buhmann, C.R. Becker, and G. Landwehr, *Phys. Rev. B* 63, 245305 (2001).
  - [7] X. C. Zhang, K. Ortner, A. Pfeufer-Jeschke, C.R. Becker, and G. Landwehr, *Phys. Rev. B* 69, 115340 (2004).
  - [8] Y.S. Gui, C.R. Becker, N. Dai, J. Liu, Z.J. Qiu, E.G. Novik, M. Schäfer, X.Z. Shu, J.H. Chu, H. Buhmann, and L.W. Molenkamp, *Phys. Rev. B* 70, 115328 (2004).
  - [9] Z.D. Kvon, S.N. Danilov, N.N. Mikhailov, S.A. Dvoretzky, and S.D. Ganichev, *Physica E* 40, 1885 (2008).
  - [10] K. Sakai, *Terahertz Optoelectronics* (Springer, Berlin 2005).
  - [11] *Terahertz Frequency Detection and Identification of Materials and Objects*, eds. R.E. Miles, X.-C. Zhang, H. Eisele, and A. Krotkus (Springer, 2007).
  - [12] *Terahertz Science and Technology for Military and Security Applications*, eds. D.L. Woolard, J.O. Jensen, and R.J. Hwu (World Scientific, 2007).
  - [13] T. Edwards, *Gigahertz and Terahertz Technologies for Broadband Communications (Satellite Communications)* (Artech House, 2000).
  - [14] *Terahertz Sensing Technology: Electronic Devices and Advanced Systems Technology: 1*, eds. D.L. Woolard, W.R. Loerop, and M. Shur, (World Scientific, 2003).
  - [15] *Semiconductor Spintronics and Quantum Computation*, eds. D.D. Awschalom, D. Loss, and N. Samarth, in the series *Nanoscience and technology*, eds. K. von Klitzing, H. Sakaki, and R. Wiesendanger (Springer, Berlin, 2002).
  - [16] I. Zutic, J. Fabian and S. Das Sarma, *Rev. Modern Phys.* 76, 323 (2004).
  - [17] *Spin Physics in Semiconductors*, ed. M.I. Dyakonov, in

- the Springer series in solid state sciences, eds. M. Cardona, P. Fulde, K. von Klitzing, R. Merlin, H.-J. Queisser, H. Stormer (Springer, Berlin, 2008).
- [18] V. S. Varavin et al., *Proceedings SPIE* 381, 5136 (2003).
- [19] G. M. H. Knippels, X. Yan, A. M. MacLeod, W. A. Gillespie, M. Yasumoto, D. Oepts, and A. F. G. van der Meer, *Phys. Rev. Lett.* 83, 1578 (1999).
- [20] B. Wittmann, S. N. Danilov, Z. D. Kvon, N. N. Mikhailov, S. A. Dvoretsky, R. Ravash, W. Prettl, and S. D. Ganichev *arXiv cond-mat: 0708.2169* (2007).
- [21] I. D. Yaroshetskii and S. M. Ryvkin, *The Photon Drag of Electrons in Semiconductors* (in Russian), in *Problems of Modern Physics* ed. V. M. Tuchkevich and V. Ya. Frenkel (Nauka, Leningrad, 1980), pp. 173-185 [English translation: *Semiconductor Physics*, ed. V. M. Tuchkevich and V. Ya. Frenkel (Cons. Bureau, New York, 1986) pp. 249-263].
- [22] A. F. Gibson and M. F. Kimmitt, *Photon Drag Detection, in Infrared and Millimeter Waves*, Vol. 3, *Detection of Radiation*, ed. K. J. Button (Academic Press, New York, 1980), pp. 181-217.
- [23] We note that in Ref. 2 applying GaAs structures made of thirty QWs we observed  $\sim 3$  mV/kW at  $\lambda = 148$  nm corresponding to 0.1 mV/kW for a single QW.
- [24] E. L. Ivchenko and G. E. Pikus, *Superlattices and Other Heterostructures. Symmetry and Optical Phenomena* (Springer, Berlin, 1997).
- [25] V. A. Shalygin, H. Diehl, Ch. Hermann, S. N. Danilov, T. Herrle, S. A. Tarasenko, D. Schuh, Ch. Gerl, W. Wegscheider, W. Prettl and S. D. Ganichev, *JETP Lett.* 84, 570 (2006).
- [26] S. D. Ganichev, U. Rossler, W. Prettl, E. L. Ivchenko, V. V. Bel'kov, R. Neumann, K. Brunner, and G. Abstreiter, *Phys. Rev. B* 66, 075328 (2002).
- [27] A. V. Andrianov, E. V. Beregulin, S. D. Ganichev, K. Yu. G. Lukh, and I. D. Yaroshetskii, *Pis'ma Zh. Tekh. Fiz.* 14, 1326 (1988) [*Sov. Tech. Phys. Lett.* 14, 580 (1988)].
- [28] M. Born, and E. Wolf, *Principles of Optics* (Pergamon Press, 1970).
- [29] V. M. Asnin, A. A. Bakun, A. M. Danishevskii, E. L. Ivchenko, G. E. Pikus, and A. A. Rogachev, *Pis'ma ZhETF* 28, 80 (1978) [*Sov. JETP Lett.* 28, 74 (1978)].
- [30] E. L. Ivchenko, and G. E. Pikus, *Pis'ma ZhETF* 27, 640 (1978) [*Sov. JETP Lett.* 27, 604 (1978)].